Technical Journal
River Research Institute ISSN: 1606-9277

QUANTIFICATION AND SPATIOTEMPORAL EVOLUTION OF TIDAL ASYMMETRY IN THE SIBSA-PUSSUR ESTUARY: A HARMONIC ANALYSIS APPROACH

M. N. Kadir[1*] and T. Naher[2]

Abstract

Tidal asymmetry in deltas, resulting from the interaction between astronomical tides and nonlinear tidal processes in shallow water, plays a crucial role in sediment transport within estuaries. Quantifying tidal asymmetry is vital for understanding the factors contributing to long-term morphological changes. This study applies the harmonic analysis method (T_tide) to examine the spatiotemporal evolution of tidal asymmetry in the Sibsa-Pussur (SP) estuary of the GBM delta, considering strongly variable river discharge conditions. Data required for analysis is collected from the results of a hydrodynamic model for 1978, 1988, 2000, and 2011. The study focuses on eight main tidal constituents (M2, M4, M6, K1, S2, O1, MS4, MSf). Tidal duration asymmetry and peak current asymmetry are determined, quantifying tidal asymmetry based on amplitude ratios and phase differences. The findings reveal that the SP estuary becomes increasingly flood dominant over time, with the Pussur River exhibiting greater flood dominance in tidal asymmetry compared to the Sibsa River. Incorporating morphological changes into the model could enhance results and provide a more accurate understanding of the sedimentation issues in the SP estuary.

Keywords: *Harmonic analysis, Morphological changes, Sibsa-Pussur Estuary, Spatiotemporal evolution, Tidal asymmetry, Tidal constituent.*

Introduction

Deltas have become desirable to inhabit due to their fertile land, abundant fisheries, and ecological and economic value (Guo *et al*., 2016). The high population density in these regions necessitates the implementation of various infrastructural projects for flood protection and land reclamation for agricultural and other purposes. Typical measures include polderization and the construction of dams and barrages for the diversion of river water for irrigation. Unfortunately, such reclamation projects often lead to a host of environmental problems, including the loss of biodiversity, deterioration of coastal water quality, and depletion of fishery resources (Son and Wang, 2009). The direct consequences of these human interventions are the prevention of natural land elevation and the onset of subsidence (Li *et al*., 2010). Additionally, embankments alter the planform shape and cross-sectional geometry of tidal rivers, resulting in strongly convergent estuaries and a reduction in intertidal area (Stark *et al*., 2017).

Like other deltas, the Ganges-Brahmaputra-Meghna (GBM) delta, a thriving ecosystem at the interface of vast rivers and the Bay of Bengal, also faces significant challenges due to its densely populated nature. Understanding these complex interactions necessitates a multifaceted approach, examining the interplay between freshwater discharge variations, tidal dynamics, and their combined influence on sediment transport. This delta exhibits a distinct spatial variation in its governing processes. The eastern part is dominated by freshwater input from the mighty Ganges and Brahmaputra rivers, resulting in a significant sediment load discharged into the Bay of Bengal (Elahi *et al*., 2020; Rahman *et al*., 2014). In contrast, the western part, comprised of the Sibsa and Pussur rivers, experiences a tide-dominated regime, allowing for importing tidal sediments (Rahman *et al*., 2018; Bomer *et al*., 2019). This inherent spatial variability underscores the need for a nuanced investigation into the specific factors shaping sediment transport within each river system.

Further complicating the scenario are anthropogenic interventions like the Farakka Barrage, constructed in 1975 to divert water from the Ganges to the Hooghly River. This has significantly reduced freshwater inflow into the Gorai River, the primary source of freshwater for the western delta (Rahman and Rahaman, 2018). The combined effects of reduced freshwater discharge and other human activities have led to many problems, including channel siltation, subsidence, and even channel abandonment (Angamuthu *et al*., 2018; Wilson *et al*., 2017).

One under-investigated aspect with potentially significant ramifications is the role of tidal asymmetry. Tidal asymmetry is one of the critical factors influencing sediment transport within estuaries (McLachlan *et al*., 2020; Yang *et al*., 2023). Unlike perfectly balanced tides, estuaries often experience flood currents with greater strength or duration compared to ebb currents. This asymmetry plays a significant role in determining the net direction and volume of sediment transport (Dronkers, 1986; Friedrichs and Aubrey, 1988; Jiang *et al*., 2011; Speer and Aubrey, 1985). In flood-dominant systems, stronger flood currents act like an import mechanism, bringing in more sediment than the ebb flow can remove. This can lead to a gradual infilling of estuaries over time. Conversely, ebb-dominant systems, with stronger ebb currents, tend to promote erosion and can deepen channels within the estuary. Understanding the type of tidal asymmetry present within a specific estuary is crucial for predicting its morphological evolution and the potential consequences for human infrastructure and coastal stability.

This research aims to elucidate the role of tidal asymmetry in shaping the contrasting behavior of the Sibsa and Pussur rivers. We hypothesize that historical changes in river discharge patterns and anthropogenic interventions may have altered the degree of tidal asymmetry within each system, influencing the direction and volume of sediment transport. By employing a hydrodynamic model and analyzing historical data, we will assess how changes in tidal asymmetry can explain the observed contrasting behavior of these rivers. This investigation will improve our understanding of the complex interplay between tides, freshwater discharge, and sediment transport in the GBM delta and provide valuable insights for sustainable management strategies to ensure the future navigability of these vital waterways. Through this research, the following questions will be answered.

[1] Department of Agricultural Engineering, Sher-e-Bangla Agricultural University, Dhaka, Bangladesh.
[*] Corresponding Author (E-mail: mnkadir@sau.edu.bd)
[2] Hydraulic Research Directorate, River Research Institute, Faridpur-7800, Bangladesh.

- How has tidal asymmetry developed in the Sibsa-Pussur estuary?
- What are the differences in tidal asymmetry between the Sibsa and Pussur rivers?

Methodology

Study Site

The western part of the lower GBM delta is considered for this study. This part is characterized as an extensive system of tide-dominated rivers (distributaries of the Ganges). The two main rivers in this part are Sibsa and Pussur Rivers. These are connected to the Ganges by the Gorai and partly by the Madhumoti and the Arial Kha rivers (**Fig. 1**). So, the flow in these systems directly depends on the Ganges River flow. The second-largest seaport of Bangladesh, known as Mongla seaport (approximately 132 km upstream from the sea), is located on the east bank of the Pussur River (**Fig. 1**). Since its establishment in 1950, this port has been playing an important role in international trade, national defense, and commerce of the country (Islam and Haider, 2016). Maintaining the navigability (at least 7.5 m navigable draft) of these rivers is necessary to keep this port active throughout the year. Because of that, several dredging efforts have been made to restore the navigability of the Pussur River (Rahman and Ali, 2018). The construction of polders is also present in this system. In 1960, the East Pakistan Water and Power Development Authority (called EP-WAPDA at that time, now known as BWDB) constructed over 139 polders (4000 km of embankments) across the entire coastal belt of Bangladesh (BWDB, 2013). These polders were built to protect the land from coastal flooding and storm surges and help achieve food security through better water control. In the southwestern part alone, about 1566 km of embankments (polders) were constructed (BWDB, 2013). Therefore, many anthropogenic interventions have affected the natural system of this area over the past five decades. This system is also crucial for the presence of the mangrove forest "Sundarbans" (**Fig. 1**). A significant part of the system runs through this forest. These extensive vegetated areas also have an enormous influence on tidal propagation.

Data processing approach

Data used in this study were obtained from secondary sources, primarily from the Bangladesh Inland Water Transport Authority (BIWTA) and the Bangladesh Water Development Board (BWDB). The BIWTA collects water level (WL) data through an automated gauge at 30-minute intervals, while the BWDB manually records high and low tide WL readings daily. Within the study area, there are two BIWTA WL measuring stations: Hiron Point, with data available from 1977 to 2015, and Mongla, with data available from 2000 to 2015 but with some missing values. The BWDB-operated Rupsha station inland has data from 1981 to 2012. However, it should be noted that the available data needed to be more sufficient for conducting a tidal analysis. Therefore, a calibrated hydrodynamic model developed by Deltares (Deltares, 2014) has been used to generate the required data for the analysis.

Tidal Analysis

Tidal analysis is necessary to determine the tidal asymmetry of a system. Harmonic analysis is the most common tidal analysis method, which provides quantitative metrics to analyze the tides. A least-squares tidal analysis (T_tide) (Pawlowicz *et al*., 2002) separates the main tidal constituents' amplitudes and phases. Before using the model output in tidal analysis, removing the high-frequency signal from the time-series data is required to get a more accurate tidal analysis result. The Godin filter was used to remove the high-frequency signal (Godin, 1972) for both the WL time-series data (**Fig. 2a**) and the velocity (both "u" and "v" components) time-series data (**Fig. 2b**).

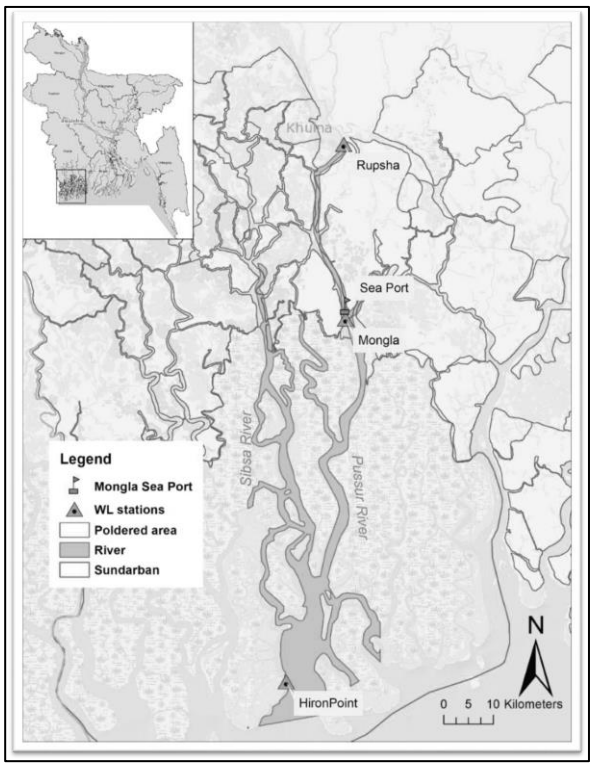

Fig. 1. Location map of the study area.

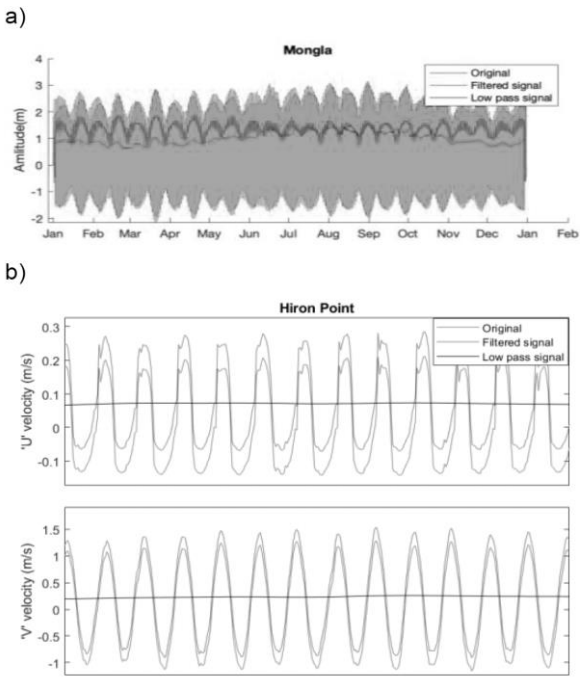

Fig. 2. Godin-filtered time series a) water level at Mongla, b) Expanded velocity time series at Hiron Point station.

a)

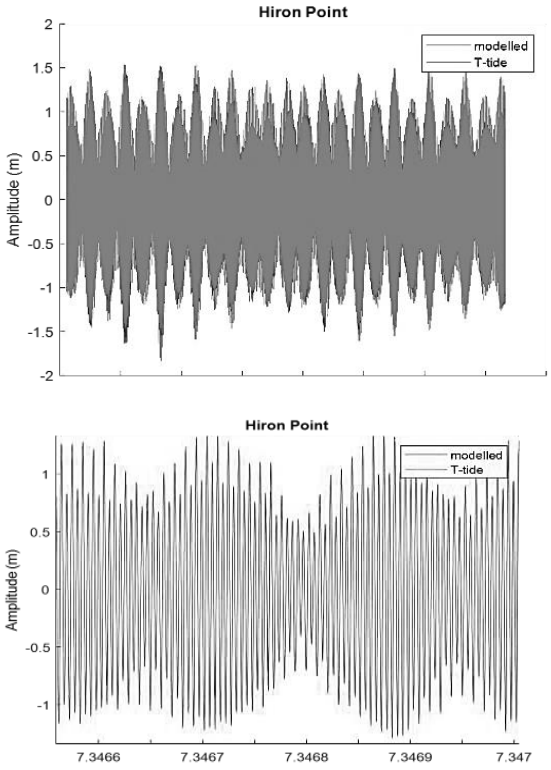

b)

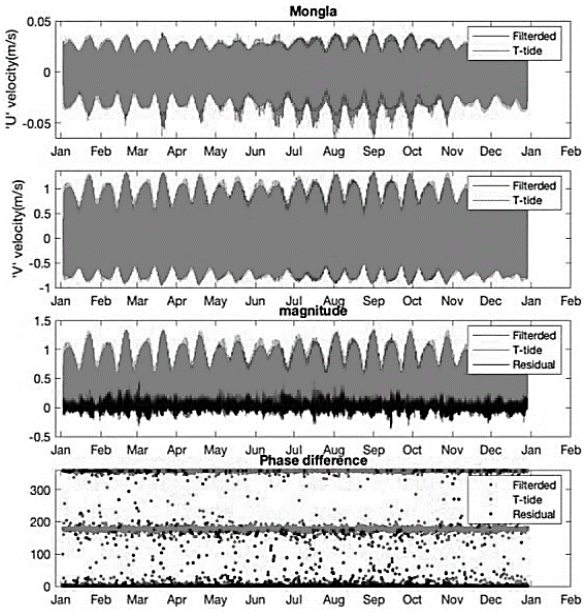

Fig. 3. Outputs of T_tide a) water level series at Hiron Point, and b) velocity time series data at Mongla station for the analysis period 2011.

According to Godin (1972), this function applies a three-step low-pass filter to a time series to remove the higher-frequency signals and obtain the residual signal. After getting the filtered time series value, the T_tide function was used for the Harmonic analysis. T_tide uses an equilibrium tide model to obtain frequencies of tidal constituents, then fits each of these constituents to the provided time series and finds each constituent's best-fit phase.

T_tide models the tidal heights ζ as

$$\zeta(t) = f_{0,0} + \sum_{i=1}^{n} [f_{1,i}\cos(\omega_i t) + f_{2,i}\sin(\omega_i t)]$$

Where t is time, ω_i is the frequency of an individual tidal constituent, and $f_{0,0}$, $f_{1,i,}$ & $f_{2,i}$ are unknown coefficients to be determined by regression analysis using observations (Pawlowicz *et al*., 2002).

The T_tide function is a powerful tool for analyzing scalar data, such as heights (**Fig. 3a**), and complex data, such as velocity (**Fig. 3b**). This model makes it possible to generate the depth-averaged velocity at a specific observation point, represented by complex data with "U" and "V" components. As all observation points are situated on the thalweg of the river, the depth-averaged velocity of the corresponding observation point is a reliable indicator of the entire cross-section. During harmonic analysis, the T_tide function calculates the magnitude of the complex data as "U" plus the square root of negative one time "V" (where "U" refers to eastward velocity and "V" refers to northward velocity) (Pawlowicz *et al*., 2002). **Fig. 3** showcases the output obtained from T_tide for the analysis period of 2011, with the model prediction fitting well with the filtered data (**Fig. 3a**).

Results

River Characteristics

A total of 21 observation points (OPs) have been selected for the Sibsa and Pussur River models, with 12 OPs located in the Pussur system and 8 OPs in the Sibsa system. The Hiron Point OP is common to both rivers and all OPs are situated on the thalweg of the river. Fig. 4 depicts the model bathymetry of the respective OPs, providing a clear illustration of the river depth and width.

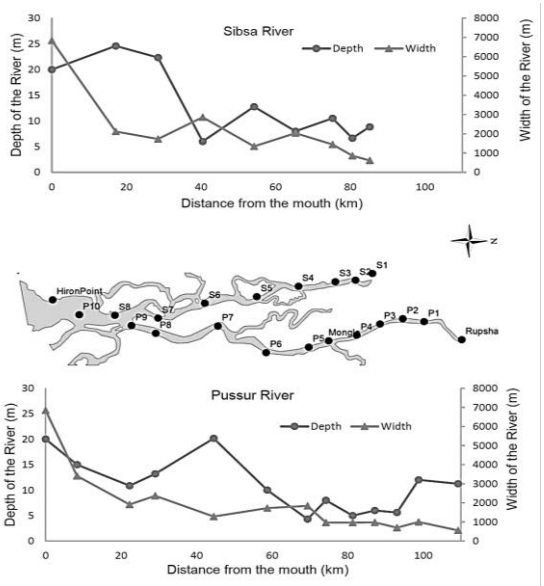

Fig. 4. River characteristics (Width and Depth) against distance from the mouth of the sea.

The rivers appear to be converging as their width decreases towards the landward direction. Upon analyzing their depths, it is evident that Sibsa holds a slightly deeper channel than Pussur. However, both rivers exhibit a decrease in depth, with Sibsa experiencing a drop at the 40km mark, and Pussur showing a sudden rise at 45km. Interestingly, the depth of Pussur begins to increase again after approximately 93km.

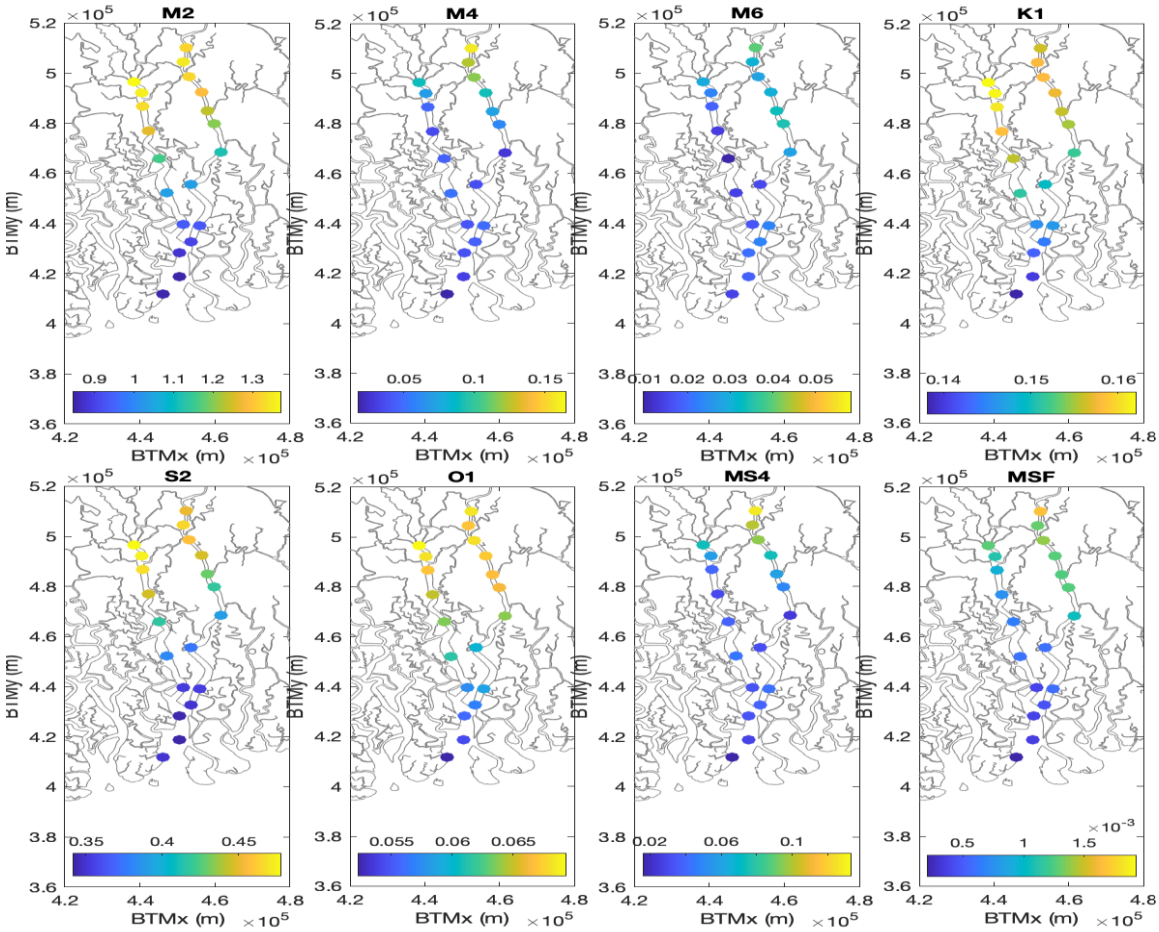

Fig. 5. Spatial variation of the vertical tidal amplitudes (M2, M4, M6, K1, S2, O1, MS4, and MSf) for the 2011 tidal analysis.

Asymmetry of the vertical tide

Spatial variation of tidal amplitudes: Like other semi-diurnal estuaries, tidal asymmetry in the Sibsa-Pussur (SP) estuary can be related to M2, S2, K1, O1, M4, M6, MS4, MSf, which are further analyzed here. M2 is the most dominant tidal constituent in the SP system, followed by S2, K1, and MS4 (**Fig. 5** and **Fig. 6**). Besides that, M4 is also considered because it is the first harmonic of M2 and dominates in many estuaries. The tidal asymmetry can also be affected by the sixth-diurnal tide M6 in some, mainly semi-diurnal estuaries. Near the coast, the effects of the fortnightly tide MSf are limited compared with those of the main diurnal and semi-diurnal tides. **Fig. 5** shows how the amplitudes of these eight constituents enlarge in the landward direction. However, the enlargement rate differs in these two rivers (**Fig. 6a** and **Fig. 6b**). The geometric convergence and decreasing depth of the Sibsa and Pussur rivers (**Fig. 5**) may gradually increase tidal amplitudes towards the estuary's landward direction.

Focusing on the main diurnal constituents K1 and O1, the T_tide results show that the variations of the mean amplitudes are in the range of 0.19–0.23 m and 0.05–0.08 m, respectively, among the different stations. The mean amplitudes of the main semi-diurnal constituents M2 and S2 range between 0.8–1.35 m and 0.28–0.4 m, respectively (**Fig. 6**). The largest amplitudes are found at the stations around the rivers' landward direction, where the poldered areas start (**Fig. 1**). The S2 amplitude is about one-third of the M2 amplitude. The narrowing of the rivers also enhances the overtides and compound tides, such as M4, MS4, and M6. The peak values of M4, MS4, and M6 amplitudes are 0.17 m, 0.12 m, and 0.06 m, respectively (**Fig. 6**). There is also a landward increase of the MSf amplitude throughout the estuary. However, compared to other constituents, the contribution from the MSf is relatively small to the tide. Two main channels are identified within the SP estuary: the Sibsa and Pussur channels. For these two channels, the along-channel variations of the mean tidal amplitudes of eight main constituents are shown in **Fig. 6a** and **Fig. 6b**.

M2 is the most dominant tide in both cases, followed by the S2, K1, MS4, M4, O1, M6, and MSf. M2 has a similar amplitude until the bifurcation point (about 13 km from the mouth of the ocean) of the two rivers; from that point onward, the trends increase. At around 93km of the Pussur channel, there was a downward trend for the M2 and S1 amplitudes. The possible reason for this change is probably the presence of interconnected channels at that point (**Fig. 1**). This may cause scouring and increase the depth (**Fig. 4**), leading to a decrease in M2 and an increase in M4.

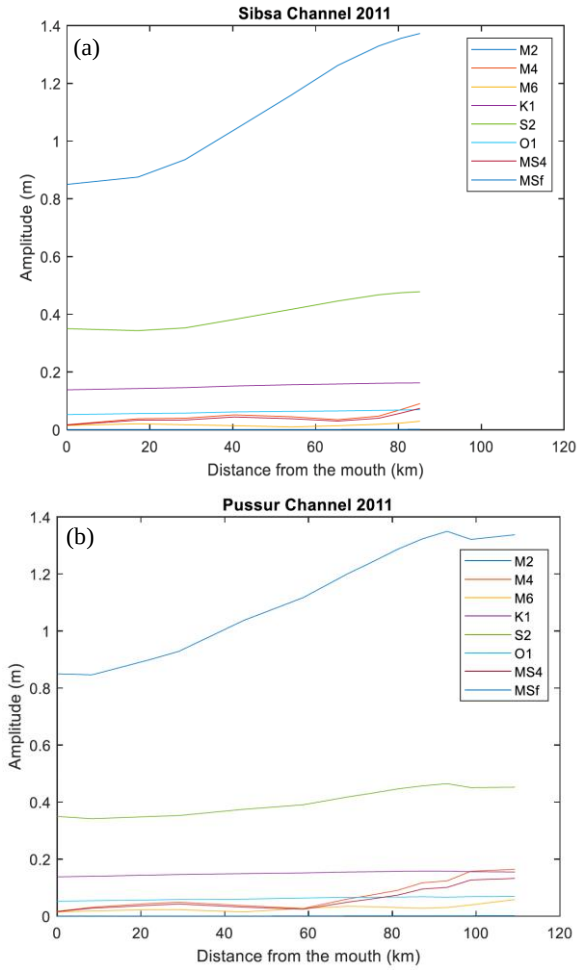

Fig. 6. Longitudinal profiles of mean tidal amplitudes of main constituents (M2, M4, M6, K1, S2, O1, MS4, MSf) along the a) Sibsa channel and b) Pussur channel in the SP estuary during 2011.

Temporal Variation of Tidal Amplitude: From 1978 to 2011, four different years (1978, 1988, 2000, and 2011) chose to run the model to mimic the temporal variation of over 33 years. The choice of the year depends on data availability and hydrological characteristics. 1978 is the earliest available data year, 1988 is the most flooded year, 2000 is the driest year, and 2011 is the latest available data and model-validating year. **Fig. 7** shows the model predictions of amplitude ratios along the Sibsa and Pussur channels between 1978 and 2011. **Fig. 7a** and **Fig. 7b** show that the Pussur channel's tidal asymmetry is more robust than the Sibsa channel. There is a slight drop at 65km for the Sibsa channel and around 60 km for the Pussur channel. Among the years, 1988 shows the strongest tidal asymmetry, followed by 2000, 1978, and 2011 for the Sibsa channel and 1978, 1988, and 2011 for the Pussur channel.

Nature of the Tidal Asymmetry

The phase difference calculations can determine whether the system is flood-dominant or ebb-dominant (2φ2- φ4). In the case of asymmetry of the horizontal tide, a system is called flood dominant when the phase difference lies between 0°-90° & 270°- 360°. From 90°-270°, represent the system as ebb dominant. The system is known as the symmetric tide if the phase difference is close to 90° or 270° (-90°). So farther from these two points will represent a more asymmetric tide. For the SP estuary, phase differences are calculated from the tidal analysis of horizontal tide (**Fig. 8**) and vertical tide (**Fig. 9**) for the years 1978, 1988, 2000, and 2011.

Peak current asymmetry:

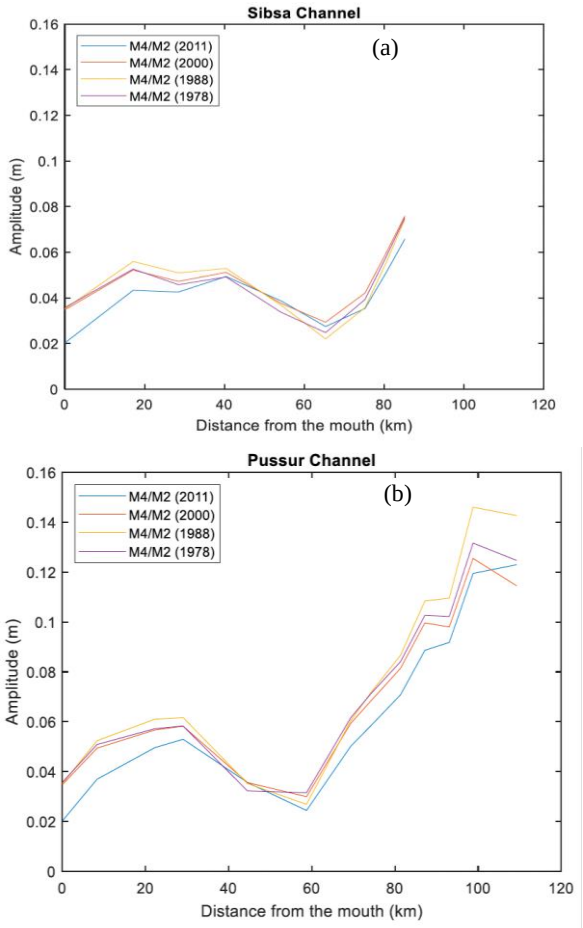

Fig. 7. The evolution of the amplitude ratio of the M2 and M4 (a & b) tidal constituent for the asymmetry of the vertical tide, derived from the model, along the Sibsa-Pussur channel between 1978 and 2011.

Fig. 8 shows the peak current asymmetry of the Sibsa (dotted line) and Pussur (solid line) rivers, along with the longitudinal profile and four different years of temporal variation. In the Sibsa channel, the temporal variations of the tidal asymmetry are not that much, except for the first point and at 30km (**Fig. 8**). However, the spatial variations are significant. Initially, it seems to be ebb dominant till 30 km, then goes close to the flood dominant to symmetric. After 80 km, the asymmetry becomes maximum flood dominant.

On the other hand, in the Pussur channel, there are some temporal variations along the river at 23 km, 45 km, and 93 km (**Fig. 8**). From 0 to 40km, recent years show close to ebb dominance. However, the rest of the river shows flood dominance. The asymmetry towards the longitudinal profile of the Sibsa River also shows flood dominance in most of the points (**Fig. 8**).

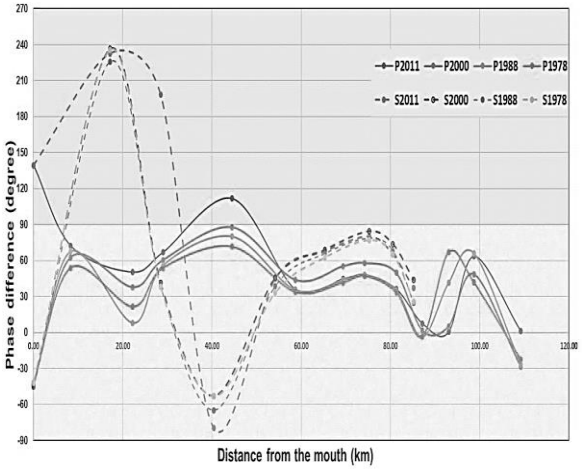

Fig. 8. Comparison of asymmetry of the horizontal tide between the Sibsa and the Pussur channel.

Tidal duration asymmetry:

Fig. 9 shows that the Sibsa channel shows more symmetrical behavior considering the tidal duration asymmetry.

In contrast, the Pussur has become more flood-dominant over time and is moving toward the landward direction. The central part of the Sibsa River (from 30 to 60 km) is symmetric or slightly ebb-dominant; afterward, it becomes flood-dominant. Whereas the Pussur behaves differently, it shows maximum flood dominant asymmetry in the central (around 60km). Afterward, it stayed at maximum flood dominance almost throughout the rest of the channel. From 0 to around 40km, Pussur behaves the same as Sibsa, becoming symmetric from the flood dominance asymmetry.

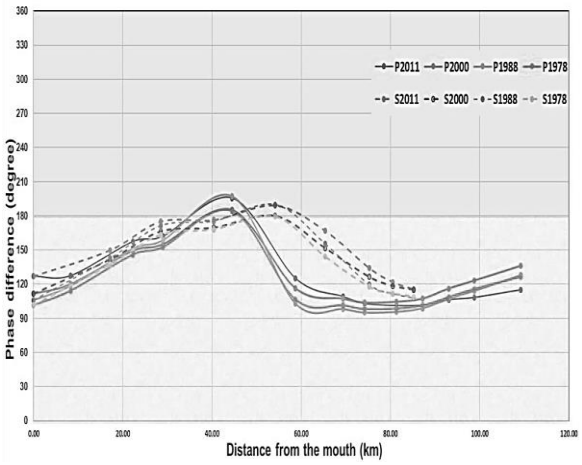

Fig. 9. Comparison of asymmetry of the vertical tide between the Sibsa and the Pussur channel.

Discussion

As stated in the introductory section, the GBM delta encounters a significant obstacle due to continuous sedimentation in the Sibsa-Pussur (SP) estuary system. This predicament is exacerbated by the sediment filling and decreased navigability of the adjacent peripheral rivers. Although human interventions may contribute, our emphasis is only on the dynamic relationship between tidal asymmetry and natural geomorphological processes.

Hoitink *et al*., (2017) suggest in their study that flood-dominant tidal asymmetry in tide-dominated deltas like the western GBM delta can lead to a dominance of inland sediment transport over river discharge and seaward sediment transport. This phenomenon essentially traps sediment within the estuary, causing aggradation (accumulation). Our findings also support this notion. The SP estuary exhibits characteristics of increasing flood dominance over time. The stronger flood currents compared to ebb currents precisely match the conditions described by Hoitink *et al.* (2017) for flood-dominant sediment transport and accumulation.

However, an exciting anomaly exists within the SP system. While the overall trend suggests flood dominance and sedimentation, a specific 20 km stretch of the Sibsa River exhibits ebb dominance (**Fig. 8**). This localized ebb dominance explains the observed erosion in this section, highlighting the erosive potential of ebb-dominant currents. The interplay between flood dominance and sedimentation creates a positive feedback loop within the SP estuary. Sedimentation alters the estuary's morphology, potentially further amplifying flood dominance. This, in turn, exacerbates the sedimentation problem, creating a self-perpetuating cycle. Understanding this feedback loop between tidal asymmetry and sedimentation is crucial for developing sustainable management strategies for the SP estuary. Numerical models and analyses of historical data can offer valuable insights into the historical evolution of tidal asymmetry and its link to morphological changes. This knowledge can then be used to devise strategies to mitigate sedimentation and ensure the long-term navigability of these vital waterways.

Future research should explore the combined effects of anthropogenic interventions and natural processes on tidal asymmetry within the SP estuary. Additionally, investigating the role of sediment grain size and channel bathymetry in influencing sediment transport dynamics can provide a more comprehensive understanding of this complex system.

Conclusion

A harmonic analysis method is applied to examine the spatiotemporal evolution of tidal asymmetry in the Sibsa-Pussur (SP) estuary of the GBM delta. The required data is generated using a hydrodynamic model (Delft-3D) for 1978, 1988, 2000, and 2011. The eight main tidal constituents (M2, M4, M6, K1, S2, O1, MS4, MSf) are considered for data analysis. The tidal duration asymmetry (as the tidal asymmetry of the vertical tide) and peak current asymmetry (as the tidal asymmetry of the horizontal tide) are determined here. The results quantify the tidal asymmetry based on the amplitude ratio and phase difference. The morphological effects are assessed based on the response of tidal asymmetry

to varying river discharge and downstream boundary conditions (changing WL), with the following main findings:

- Despite some anomalies in the peak current asymmetry, most parts of the Sibsa-Pussur system are flood-dominant. Tidal asymmetry changes are slightly symmetric, followed by maximum flood dominant asymmetry towards the delta's landward direction under the substantial effect of nonlinear interactions. The M2 and M4 amplitudes are more dominant among the other semidiurnal tides and overtides, respectively. Temporal variation in the tidal asymmetry is found very little, considering the hydrodynamical changes only.
- The Pussur channel is more flood-dominant than the Sibsa. The Sibsa channel shows more symmetrical behaviors, whereas the Pussur channel mostly shows maximum flood-dominant asymmetry. The influence of anthropogenic activities on the Pussur system is more significant than that on the Sibsa system.

Acknowledgment

This article is a rendition of the master's thesis authored by the corresponding author. The author expresses heartfelt gratitude to all the advisors involved in this project for their unwavering support and guidance throughout. Additionally, the authors sincerely thank Deltares for generously granting permission to utilize their model. Furthermore, the author acknowledges the constructive reviewer, which positively impacted the quality of this article.

References

Angamuthu, B., Darby, S. E. and Nicholls, R. J. (2018). Impacts of natural and human drivers on the multi-decadal morphological evolution of tidally-influenced deltas. *Proc. R. Soc. A.* 474(2219): 20180396. https://doi.org/10.1098/rspa.2018.0396

Bomer, E. J., Wilson, C. A. and Datta, D. K. (2019). An integrated approach for constraining depositional zones in a tide-influenced river: Insights from the Gorai River, Southwest Bangladesh. *Water*. 11(10): 2047. https://doi.org/10.3390/w11102047

BWDB. (2013). Final Report on Environmental Impact Assessment (EIA) CEIP-I. Bangladesh Water Development Board (BWDB). *(Issue January)*. https://www.bwdb.gov.bd/archive/pdf/284.pdf

Deltares. (2014). 3D/2D modeling suite for integral water solutions: Hydro-Morphodynamics. 710.

Dronkers, J. (1986). Tidal asymmetry and estuarine morphology. *Neth. J. Sea Res.* 20(2–3): 117–131.

Elahi, M. W. E., Jalón-Rojas, I., Wang, X. H. and Ritchie, E. A. (2020). Influence of seasonal river discharge on tidal propagation in the Ganges-Brahmaputra-Meghna Delta, Bangladesh. *J. Geophys. Res. Oceans.* 125(11): e2020JC016417.

Friedrichs, C. T. and Aubrey, D. G. (1988). Non-linear tidal distortion in shallow well-mixed estuaries: a synthesis. *Estuar. Coast Shelf Sci. 27(5)*: 521–545. https://doi.org/10.1016/0272-7714(88)90082-0

Godin, G. (1972). The analysis of tides. *Univ. of Toronto Press*. https://doi.org/10.1016/0025-3227(73)90070-4

Guo, S., Sun, J., Zhao, Q., Feng, Y., Huang, D. and Liu, S. (2016). Sinking rates of phytoplankton in the Changjiang (Yangtze River) estuary: A comparative study between Prorocentrum dentatum and Skeletonema dorhnii bloom. *J. Mar. Syst.* 154 (Part A): 5–14. https://doi.org/10.1016/j.jmarsys.2015.07.003

Hoitink, A. J. F., Wang, Z. B., Vermeulen, B., Huismans, Y. and Kästner, K. (2017). Tidal controls on river delta morphology. *Nat. Geosci.* 10(9): 637–645. https://doi.org/10.1038/ngeo3000

Islam, M. A. and Haider, M. Z. (2016). Performance assessment of Mongla seaport in Bangladesh. *Int. J. Transp. Eng. Tech.* 2(2): 15-21. https://doi.org/10.11648/j.ijtet.20160202.11

Jiang, A. W., Ranasinghe, R., Cowell, P. and Savioli, J. C. (2011). Tidal asymmetry of a shallow, well-mixed estuary and the implications on net sediment transport: A numerical modelling study. *Aust. J. Civ. Eng.* 9(1): 1–18.

Li, K., Liu, X., Zhao, X. and Guo, W. (2010). Effects of reclamation projects on marine ecological environment in Tianjin Harbor Industrial Zone. *Procedia Environ. Sci.* 2: 792–799. https://doi.org/10.1016/j.proenv.2010.10.090

McLachlan, R. L., Ogston, A. S., Asp, N. E., Fricke, A. T., Nittrouer, C. A. and Gomes, V. J. C. (2020). Impacts of tidal-channel connectivity on transport asymmetry and sediment exchange with mangrove forests. *Estuar. Coast Shelf Sci.* 233: 106524.

Pawlowicz, R., Beardsley, B. and Lentz, S. (2002). Classical tidal harmonic analysis including error estimates in MATLAB using TDE. *Comput. Geosci.* 28(8): 929–937. https://doi.org/10.1016/S0098-3004(02)00013-4

Rahman, M., Dustegir, M., Karim, R., Haque, A., Nicholls, R. J., Darby, S. E., Nakagawa, H., Hossain, M., Dunn, F. E. and Akter, M. (2018). Recent sediment flux to the Ganges-Brahmaputra-Meghna delta system. *Sci. Total Environ.* 643: 1054–1064.

Rahman, M. Z., Beg, M. N. A. and Khan, Z. H. (2014). Sediment budget of Meghna Estuary. *Tech. J. River Res. Inst.* 12(1): 106–118. https://doi.org/10.5281/ZENODO.3351639

Rahman, Md. M. and Rahaman, M. M. (2018). Impacts of Farakka barrage on hydrological flow of Ganges river and environment in Bangladesh. *Sustain. Water Resour. Manag.* 4(4): 767–780.

Rahman, M. M. and Ali, M. S. (2018). Potential causes of navigation problem in Pussur river and interventions for navigation enhancement. *4th Int. Conf. Civil Eng. Sust. Dev.* (ICCESD-2018).

Son, S. and Wang, M. (2009). Environmental responses to a land reclamation project in South Korea. *Eos*, 90(44): 398–399. https://doi.org/10.1029/2009EO440002

Speer, P. E. and Aubrey, D. G. (1985). A study of non-linear tidal propagation in shallow inlet/estuarine systems Part II: Theory. *Estuar. Coast Shelf Sci.* 21(2): 207–224. https://doi.org/10.1016/0272-7714(85)90097-6

Stark, J., Smolders, S., Meire, P. and Temmerman, S. (2017). Impact of intertidal area characteristics on estuarine tidal hydrodynamics: A modelling study for the Scheldt Estuary. *Estuar. Coast Shelf Sci.* 198: 138–155. https://doi.org/10.1016/j.ecss.2017.09.004

Yang, Z., Liang, Z., Ren, Y., Ji, D., Luan, H., Li, C., Cui, Y. and Lorke, A. (2023). Influence of asymmetric tidal mixing on sediment dynamics in a partially mixed estuary. *Acta Oceanologica Sinica*, 42(9): 1-15.

Wilson, C., Goodbred, S., Small, C., Gilligan, J., Sams, S., Mallick, B. and Hale, R. (2017). Widespread infilling of tidal channels and navigable waterways in the human-modified tidal delta plain of southwest Bangladesh. *Elem. Sci. Anth.* 5: 78. https://doi.org/10.1525/elementa.263